Biosensors and Bioelectronics 135 (2019) 1–7

Contents lists available at ScienceDirect

Biosensors and Bioelectronics

journal homepage: www.elsevier.com/locate/bios

A paper-based electrochemical immunosensor with reduced graphene oxide/thionine/gold nanoparticles nanocomposites modification for the detection of cancer antigen 125

Yan Fan[a,*], Shengyu Shi[b], Junshuang Ma[a], Yaohua Guo[a]

[a] Intelligence and Information Engineering College of Tangshan University, Tangshan, 063000, China
[b] General Cargo Branch of Qinhuangdao Port Company Limited, Qinhuangdao, 066000, China

ARTICLE INFO

Keywords:
Paper-based
Electrochemical
Immunosensor
rGO/Thi/AuNPs nanocomposites
Point-of-care testing

ABSTRACT

A paper-based electrochemical immunosensor was developed for the detection of cancer antigen 125 (CA125) by screen-printing technique. The reduced graphene oxide/thionine/gold nanoparticles (rGO/Thi/AuNPs) nanocomposites were compounded and coated onto the working electrode of immunosensor for CA125 antibody (anti-CA125) immobilization and detection signal amplification. The detection principle was based on the fact that the immunocomplex formed by specify binding of CA125 antibody and antigen could reduce the current response of thionine, which was proportional to the corresponding concentration of CA125 antigen. The immunoassay results showed that the linear range of CA125 was from 0.1 U mL^{-1} to 200 U mL^{-1} with the limit of detection (LOD) of 0.01 U mL^{-1} at signal to noise of 3. Quality control serum samples measured by our proposed immunosensor showed acceptable agreement with traditional ELISA method with the relative error less than 8.05%. The immunosensor exhibited good electrochemical performance with high reproducibility, reliability, stability and accuracy. The proposed immunosensor could be used for the determination of CA125 and had the potential for point-of-care testing (POCT) of other tumor marker.

1. Introduction

Recently, immunoassay of tumor marker has aroused extensive attention due to its advantages in early diagnosis of diseases and evaluation of surgical prognosis (Babamiri et al., 2017; Gasparotto et al., 2017; Johariahar et al., 2015; Li et al., 2014a; 2014b; Wu et al., 2014). Cancer antigen 125 (CA125) is a kind of tumor marker, which is closely related to ovarian cancer (Al-Ogaidi et al., 2014). The cut-off value of CA125 is less than 35 U mL^{-1} in healthy human serum. The CA125 levels in more than 80% of advanced ovarian cancer patients are higher than that in healthy human serum (Nguyen et al., 2013; Santillan et al., 2005). Combined with other protein biomarkers, CA125 can be used for the early diagnosis of ovarian cancer. The elevated levels of CA125 have also been found in patients with lung cancer, endometrial cancer and breast cancer (Guo et al., 2003; Francis, 2016). Thus, the detection of CA125 with low detection limit and high sensitivity plays an important role in the clinical diagnosis of these cancers.

Since paper has the advantages of low cost, disposability, good biocompatibility and easy availability, it becomes the first choice for the fabrication of immunosensor (Nery and Kubota, 2013). Many research groups have made great efforts on the development of paper-based immunosensors in recent decades (Chu et al., 2017; Wang et al., 2016; Fan et al., 2016; Yan et al., 2014; Santhiago and Kubota, 2013; Martinez et al., 2008). Numerous fabrication methods of paper-based immunosensors have been presented including wax printing, UV photolithography, plasma treatment, screen printing and laser treatment (Hu et al., 2015; Yan et al., 2014; Songjaroen et al., 2012; Zhang and Zha, 2012; Dungchai et al., 2011). Among these methods, screen printing has the advantages of low cost and simple fabrication process, which can be used for mass production of paper-based immunosensors (Wang et al., 2016; Li et al., 2014a; 2014b; Wu et al., 2014). The paper-based immunosensor is very suitable for point-of-care testing (POCT) of tumor markers with the features of environmental compatibility and simple fabrication method (Bruzewicz et al., 2008; Nery and Kubota, 2013). Lots of methods have been developed for the detection of different analytes such as electrochemiluminescent immunoassay (Babamiri et al., 2017; Li et al., 2013), colorimetric method (Olkkonen et al., 2010; Klasner et al., 2010), chemiluminescent immunoassay (Chu et al., 2017; Xiao and Lin, 2015; Lei et al., 2014) and electrochemical immunoassay (Torati et al., 2017; Fan et al., 2017; Wang et al., 2016;

* Corresponding author.
E-mail address: fanfenyan@aliyun.com (Y. Fan).

https://doi.org/10.1016/j.bios.2019.03.063
Received 16 January 2019; Received in revised form 28 March 2019; Accepted 31 March 2019
Available online 05 April 2019
0956-5663/

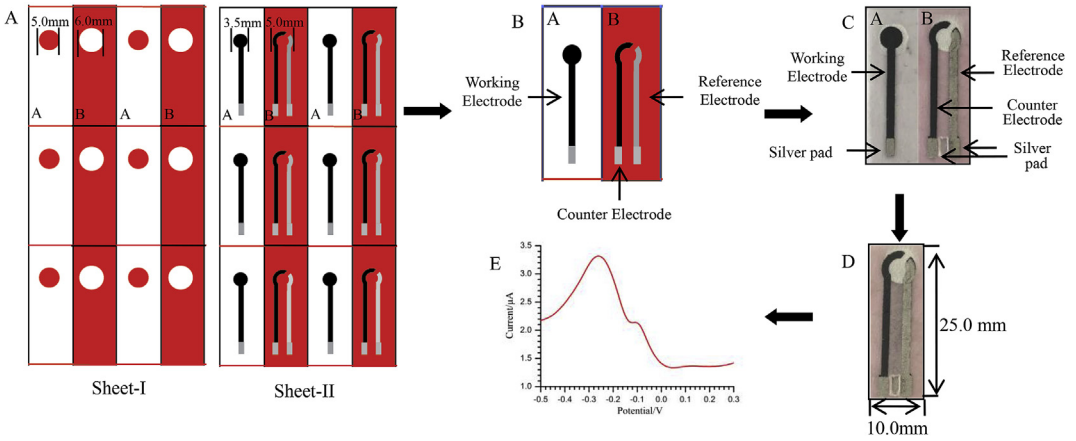

Scheme 1. The fabrication and detection process of paper-based immunosensor. (A) the screen-printed patterns for wax printing and electrodes on Sheet-I and sheet-II. Sample zone (diameter = 5.0 mm) and auxiliary zone (diameter = 6.0 mm) on paper-A and paper-B of sheet-I were designed for screen-printing of carbon working electrode, carbon counter electrode and Ag|AgCl reference electrode. The patterns of carbon working electrode (diameter = 3.5 mm), carbon counter electrode and Ag|AgCl reference electrode (diameter = 5.0 mm) were designed on paper-A and paper-B of sheet-II, respectively; (B) The single immunosensor of three electrodes: working electrode, counter electrode and reference electrode; (C) Photograph of single fabricated immunosensor with silver pad; (D) The folded immunosensor (10.0 × 25.0 cm); (E) DPV schematic plot measured with nanocomposites modified immunosensor.

Rong et al., 2016; Wu et al., 2014; Li et al., 2014b). Among those methods, electrochemical immunoassay has received much attention due to its features such as low cost, high accuracy and sensitivity.

Different kinds of electrochemical immunosensors have been designed for the detection of tumor markers (Torati et al., 2017; Wang et al., 2016; Han et al., 2013; Peng et al., 2014). The important issue for the detection of tumor makers is to establish a proper electrochemical immunoassay method. Many methods have been made for antibody immobilization and signal amplification (Torati et al., 2017; Wang et al., 2016; Rong et al., 2016; Wu et al., 2014). Nanomaterials are commonly utilized to modify the electrode of immunosensor for immobilizing antibody and amplifying signal. Owing to its excellent conductivity, high specific surface area and good biocompatibility, graphene is considered as a promising nanomaterial in biomedical domain (Bolotin et al., 2008). Graphene can be prepared as reduced gaphene oxide (rGO) by oxidation reduction for signal amplification. Metal particles such as gold nanoparticles (AuNPs) are also usually chosen to amplify signal due to its good electrical properties and large specific surface area (Lu et al., 2012). Thionine (Thi), a kind of electroactive material, is used for inducing redox current response during testing. Thus, rGO, AuNPs and Thi are chosen for signal amplification and antibody immobilization in this article. The rGO/Thi nanocomposites are synthesized through π-π stacking interaction between rGO and Thi molecules, which had benzene ring and could non-covalently attach to rGO (Jia et al., 2014). AuNPs are immobilized onto rGO/Thi nanocomposites via the interaction between amino groups of rGO/Thi and gold nanoparticles. The rGO/Thi/AuNPs nanocomposites are modified on the working electrode of immunosensor for antibody immobilization and signal amplification.

In this work, a novel electrochemical immunosensor was proposed for the detection of CA125 base on rGO/Thi/AuNPs nanocomposites. The immunosensor was fabricated by simple and low-cost screen-printing technique. The rGO/Thi/AuNPs nanocomposites were synthesized to modify the immunosensor. Under optimal conditions, CA125 was detected with the proposed immunosensor. The detection results showed that the proposed immunosensor had good performance and could provide a simple and rapid way for POCT of CA125.

2. Experimental

2.1. Reagents and materials

Mouse CA125 antibody, human CA125 antigen and quality control serum samples were obtained from Yuduobio Company (Shanghai, China). CA125 ELISA kit and bovine serum albumin (BSA) were got from Chundubio Company (Wuhan, China). The rGO and AuNPs were obtained from Tanfeng Graphene Science and Technology Co., Ltd. (Nanjing, China). Thi was purchased from Duly Biotech Company (Nanjing, China). Silver/silver chloride (Ag|AgCl) ink (JLL-20) was got from Shanghai Electronic Technology Company (Shanghai, China). Carbon ink (ED423 ss) was purchased from Acheson (Germany). Whatman No.1 chromatography paper (pure cellulose paper) was got from GE Healthcare Worldwide (Shanghai, China) and adjusted size in the further use. All other chemicals were of analytical grade and directly used as received.

2.2. Apparatus

All electrochemical immunoassay measurements including differential pulse voltammetry (DPV) and cyclic voltammetry (CV) were performed on a CHI 660E electrochemical workstation (CH Instrument Co., Shanghai, China). Scanning electron microscopic (SEM) images were determined with a FEI Scientific_Q250_SEM (American). A Lenovo computer was used for data collecting. Ultrapure water (resistance > 18 MΩ) was got through Michem ultrapure water apparatus (Chengdu, China).

2.3. Fabrication of paper-based immunosensor

The paper-based immunosensor was fabricated on pure cellulose paper. As shown in Scheme 1., the patterns of immunosensor were designed with Adobe Illustrate CS6. In Scheme 1(A), sheet-I and sheet-II were screen-printing patterns for wax printing and electrodes, respectively. Each immunosensor was composed of two pieces of paper with the same size (10.0 × 25.0 cm). On paper-A of sheet-I, sample zone (diameter = 5.0 mm) was designed for screen-printing of carbon working electrode. Auxiliary zone (diameter = 6.0 mm) was designed for screen-printing of carbon counter electrode and Ag|AgCl reference electrode on paper-B of sheet-I. The patterns of carbon working electrode (diameter = 3.5 mm), carbon counter electrode and Ag|AgCl reference electrode (diameter = 5.0 mm) were designed on paper-A and paper-B of sheet-II, respectively. The sheet-I and sheet-II could be divided into several single immunosensors, as shown in Scheme 1(B). The photograph of single fabricated immunosensor was shown in Scheme 1(C). A small square of paper-B was cut off to expose the lead of carbon working electrode. After folding paper-A and paper-B, immunosensor

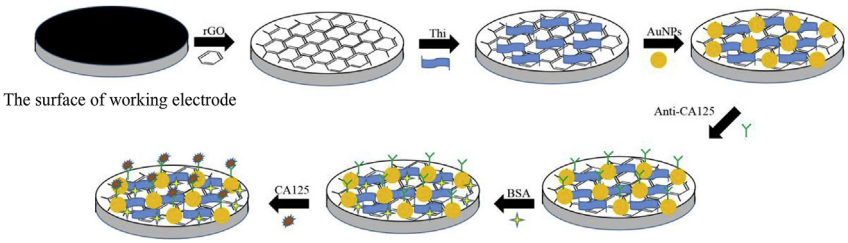

Scheme 2. The compound process of rGO/Thi/AuNPs nanocomposites.

was formed (10.0 × 25.0 cm) and the three electrodes of immunosensor were well connected in one system via filling with sample solution (20 μL), shown in Scheme 1(D). Scheme 1(E) was the DPV schematic plot measured with rGO/Thi/AuNPs nanocomposites modified immunosensor.

The fabrication process of immunosensor was described as follows. Firstly, the mask patterns of screen-printing were designed with Adobe Illustrate CS6 and sent to a local screen-printing company for creating the screens. On sheet-I, red circle in paper-A and white circle in paper-B were the hydrophilic areas for screen-printing of electrodes, while the remaining white area in paper-A and red area in paper-B were the hydrophobic area. Secondly, the solid wax was printed by rubbing through the mesh of screens (250 mesh of polyester with aluminium frame) onto the surface of pure cellulose paper. The wax-printed paper was placed in 90 °C oven for 2 min to form the hydrophobic area through fully spreading of wax into the fiber of paper. Then the prepared paper was placed in room temperature for cool (Dungchai et al., 2011). Thirdly, the carbon working electrode, carbon counter electrode and Ag|AgCl reference electrode were screen-printed with carbon ink and Ag|AgCl ink on the circles zones of paper A and paper B, respectively. The silver pads were screen-printed with silver ink to lower impedance. The screen-printed paper was dried in the 80 °C oven for 20 min for solidification. Finally, the paper was cut into single pieces and folded with double-side tape for use.

2.4. Synthesis of rGO/Thi/AuNPs nanocomposites

For synthesis of rGO/Thi/AuNPs nanocomposites, rGO/Thi nanocomposites were firstly compounded. 1 mL rGO solution (1 mg mL^{-1}) was treated with ultrasonic for 30 min and mixed with 1 mL Thi solution (2 mg mL^{-1}). The mixed solution was stirred vigorously for 24 h at room temperature. Centrifugation and fully washing with ultrapure water were adopted to get rid of non-integrated Thi molecules, then rGO/Thi nanocomposites were obtained. The obtained rGO/Thi nanocomposites were dispersed into 2 mL ultrapure water and mixed with 10 mL AuNPs solution. After stirring overnight, AuNPs nanoparticles were well connected to rGO/Thi nanocomposites. Through centrifugation and fully washing, the obtained rGO/Thi/AuNPs nanocomposites were dispersed into 1 mL 0.1% chitosan solution and stored in the fridge prior to use (Jia et al., 2014; Wang et al., 2016).

2.5. Preparation of electrochemical immunosensor

The preparation process of immunosensor was described as follows. Above all, 10 μL rGO/Thi/AuNPs nanocomposites solution was added onto the working electrode of immunosensor and put into an 50 °C oven for 15 min. Secondly, 10 μL anti-CA125 (100 μg mL^{-1}) was added onto the modified working electrode and stored at 4 °C for 6 h. Thirdly, 10 μL 1% BSA was added to the modified working electrode to refrain from non-specific adsorption and block the remaining active sites. Finally, the modified immunosensor was thoroughly washed with PBS solution and saved in the fridge at 4 °C for further use.

2.6. Electrochemical assay method of CA125

A series of CA125 antigen standard solution with different concentrations were added onto the working electrode of rGO/Thi/AuNPs/anti-CA125 modified immunosensor and incubated for 20 min at room temperature. After carefully washing with 0.1 M PBS (PH = 7.4), electrochemical measurements including CV and DPV were executed with electrochemical workstation CHI 660E. The voltage range of CV measurements were conducted from −0.55 V to 0.3 V with scan rate of 0.1 V s^{-1}. The DPV measurements were taken with scanning voltage between −0.5 V and 0.3 V, pulse amplitude of 50 mV, pulse width of 50 ms and pulse period of 1s.

Quality control serum samples of healthy persons and ovarian cancer patients were assayed with immunosensor by using ELISA method as a reference. Serum sample of uninfected health person was used as a negative control. Samples with known concentration from 2 U mL^{-1} to 64 U mL^{-1} (2 U mL^{-1}, 4 U mL^{-1}, 8 U mL^{-1}, 16 U mL^{-1}, 32 U mL^{-1}, 64 U mL^{-1}) were tested three times to get calibration curve with immunosensor and ELISA method. Eight quality control serum samples were measured three times with eight immunosensors and ELISA method. The high concentration of samples were diluted 10 times with sample diluent and the concentration was obtained through multiplying the result by 10. The comparison results were obtained between these two methods to verify the clinical potential of immunosensor.

3. Results and discussion

3.1. Theory of electrochemical immunoassay

In order to execute accurate electrochemical measurement of CA125, rGO/Thi/AuNPs nanocomposites were synthesized for antibody immobilization and signal amplification. As shown in Scheme 2., Thi molecules were non-covalently binding with rGO via π–π stacking to form rGO/Thi nanocomposites. The rGO/Thi/AuNPs nanocomposites were obtained according the theory that AuNPs nanoparticles had high affinity for the amino groups of rGO/Thi nanocomposites (Jia et al., 2014). Anti-CA125 was immobilized on the working electrode surface of rGO/Thi/AuNPs nanocomposites modified immunosensor through the interaction between the amino groups of antibody and AuNPs (Peng et al., 2014; Jia et al., 2014; Wang et al., 2016). The testing of CA125 was executed with DPV measurements. The DPV current responses decreased with the increasing concentrations of CA125, which might be attributed to the immunocomplex formed by specify binding of CA125 antibody and antigen. The formed immunocomplex acted as mass-transfer and electron-transfer blocking layer, which blocked the electron transfer tunnel and hindered the electron transfer toward the surface of electrode (Jia et al., 2014; Han et al., 2013; Wei et al., 2010; Yu et al., 2013).

3.2. Characterization and elctrochemical performance of immunosensor

In order to identify the modification of rGO/Thi/AuNPs nanocomposites on the surface of working electrode, SEM images were performed with FEI Scientific_Q250_SEM. SEM images of bare working

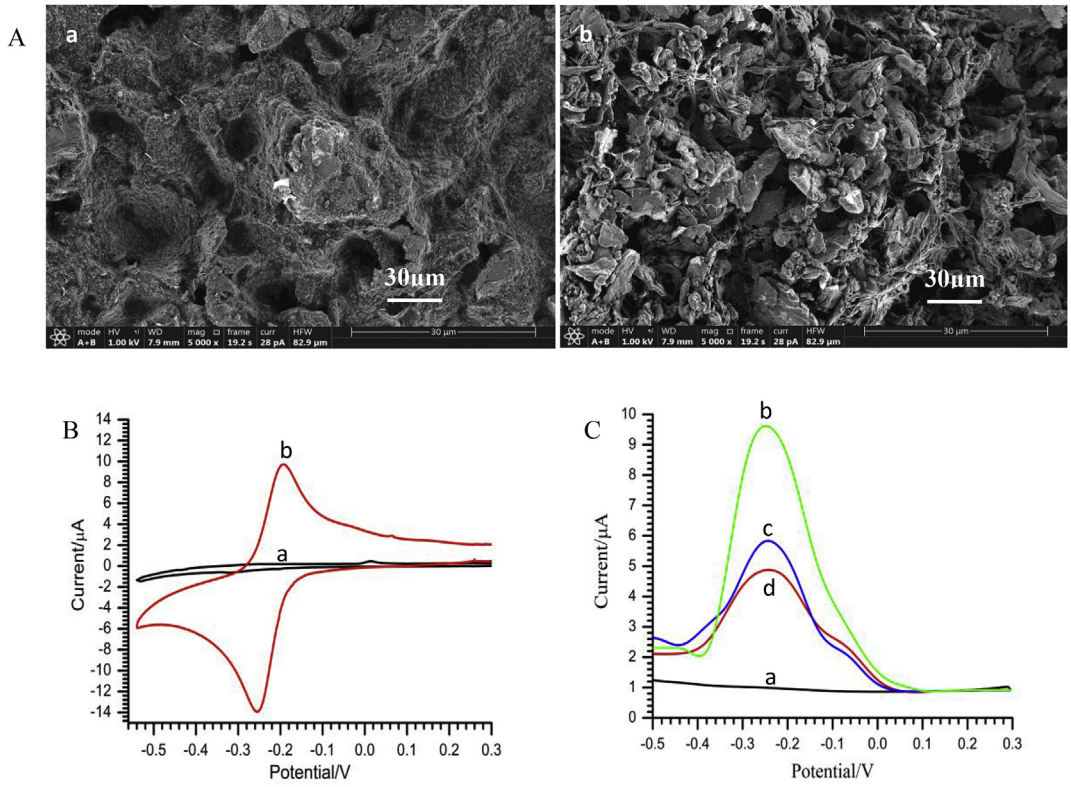

Fig. 1. SEM images and electrochemical performance of immunosensor. (A) SEM images of bare working electrode (a) and immunosensor modified with rGO/Thi/AuNPs nanocomposites (b) under the same scale (30 μm); (B) CV current responses of bare working electrode (a) and immunosensor modified with rGO/Thi/AuNPs nanocomposites (b) in 0.1 M PBS (PH = 7.4); (C) DPV current responses of bare working electrode(a), immunosensor modified with rGO/Thi/AuNPs nanocomposites (b), rGO/Thi/AuNPs/anti-CA125 (c) and rGO/Thi/AuNPs/anti-CA125/BSA (d) in 0.1 M PBS (PH = 7.4).

electrode (Fig. 1A–a) and working electrode modified with rGO/Thi/AuNPs nanocomposites (Fig. 1A-b) under the same scale (30 μm) were shown in Fig. 1A, respectively. The comparison of SEM images showed that rGO/Thi/AuNPs nanocomposites were successfully modified on the surface of working electrode with loose nanoporous structures. It could provide large specific surface area to adsorb more active molecules, thus amplify the current response.

To illustrate the performance of rGO/Thi/AuNPs modified immunosensor, CV and DPV measurements were performed in 0.1 M PBS buffer solution (PH = 7.4), shown in Fig. 1B and C, respectively. As shown in Fig. 1B, CV current responses of bare working electrode (curve a) and rGO/Thi/AuNPs nanocomposites modified immunosensor (curve b) were determined. A pair of obvious redox peak current of rGO/Thi/AuNPs modified immunosensor appeared clearly at −0.25 V and −0.19 V due to the redox activity of Thi in rGO/Thi/AuNPs nanocomposites. As shown in Fig.S1(a), the CV measurements were performed at different scan rates between 20 mV s^{-1} and 200 mV s^{-1} (20 mV s^{-1}, 50 mV s^{-1}, 100 mV s^{-1}, 150 mV s^{-1}, 200 mV s^{-1}). The anodic and cathodic peak current were in proportion to scan rate (Fig.S1(b)), indicating a surface-confined redox process (Lu et al., 2014; Peng et al., 2014). DPV current responses of bare working electrode, immunosensor modified with rGO/Thi/AuNPs, rGO/Thi/AuNPs/anti-CA125 and rGO/Thi/AuNPs/anti-CA125/BSA were 0.537 μA, 9.607 μA, 5.834 μA and 4.875 μA, respectively (curve a~d). The redox peak of rGO/Thi/AuNPs modified immunosensor (curve b) was attributed to the redox reaction of Thi in the rGO/Thi/AuNPs nanocomposites. Due to loose nanoporous structures, rGO/Thi/AuNPs nanocomposites could enlarge the surface area and markedly amplify the detection signal. The CA125 antibody could form electron-blocking layer and retard electron transfer of Thi molecules, thus DPV current response of rGO/Thi/AuNPs/anti-CA125 modified immunosensor (curve c) was lower than the DPV current response of rGO/Thi/AuNPs modified immunosensor (curve b) (Han et al., 2013). Similarly, DPV current response of rGO/Thi/AuNPs/anti-CA125/BSA modified immunosensor (curve d) further decreased due to the insulating BSA layer which hindered the electron transfer (Han et al., 2013, Lu et al., 2014). The DPV current response of rGO/Thi/AuNPs/anti-CA125/BSA modified immunosensor provided stable DPV current response because that BSA could block nonspecific adsorption and possible remaining active sites. DPV current response showed that the proposed immunosensor was successfully modified and could be adopted for the testing of different concentration of CA125.

3.3. Optimization condition for electrochemical immunoassay

3.3.1. Optimization proportion between rGO/Thi and AuNPs

In the immunoassay, rGO and AuNPs were used for signal amplification, therefore the proportion of nanomaterials affected the detection results. In the previous section, the rGO/Thi nanocomposites were synthesized firstly, so we investigated the influence of different proportion of rGO/Thi to AuNPs. 20 μL rGO/Thi dispersion was blended with various amount of AuNPs including 60 μL, 80 μL, 100 μL, 120 μL and 140 μL, the corresponding proportion was 1:3, 1:4, 1:5, 1:6 and 1:7. The DPV current responses were shown in Fig. S2. Due to good electrical feature of AuNPs, the DPV current responses rose with the increasing amount of AuNPs. Nevertheless, if excess AuNPs were added to the rGO/Thi dispersion, it would occur aggregation effect which lowered its electrical conductivity. The optimal proportion of rGO/Thi to AuNPs was 1:5 which would be used for electrochemical immunoassay of CA125.

3.3.2. Optimization incubation time of CA125 antibody and antigen

In the electrochemical immunoassay of CA125, incubation time impacted the performance of immunosensor. When CA125 antigen was add onto the immunosensor, it took some time for the specific binding

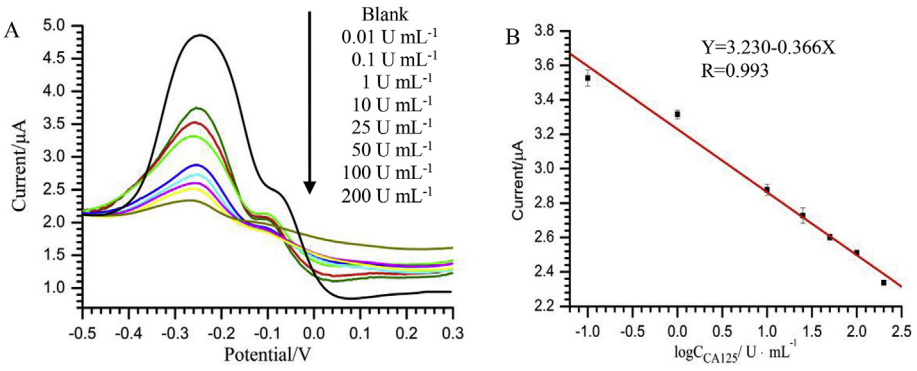

Fig. 2. DPV responses and calibration curve of immunosensor with different concentration of CA125 antigen. (A) The DPV responses of immunosensor for different concentration of CA125 from 0.01 U mL^{-1} to 200 U mL^{-1} (0.01 U mL^{-1}, 0.1 U mL^{-1}, 1 U mL^{-1}, 10 U mL^{-1}, 25 U mL^{-1}, 50 U mL^{-1}, 100 U mL^{-1} and 200 U mL^{-1}); (B) The calibration curve of immunosensor between the DPV peak current and the logarithm of different concentration of CA125 (0.1–200U mL^{-1}).

of CA125 antigen and antibody. As shown in Fig. S3, rGO/Thi/AuNPs modified immunosensor was incubated with 1 U mL^{-1} CA125 under different incubation time (10 min, 15 min, 20 min and 25 min). DPV peak current responses firstly increased with the increase of incubation time and reached the maximum at 20 min, then leveled off after 20 min, indicating the saturation binding of CA125 antigen and antibody. Hence, 20 min was chosen as the optimal incubation time in the following immunoassay.

3.4. Analytical performance of CA125

Under the optimum reaction conditions, the analytical performance of immunosensor was tested with CA125 standard solution. Each concentration of CA125 was measured three times. As shown in Fig. 2A, DPV current responses decreased along with the increase of CA125 concentration from 0.01 U mL^{-1} to 200 U mL^{-1}. The reason might be that the formation of CA125 antibody-antigen immunocomplex acted as mass-transfer and electron-transfer blocking layer, which blocked the electron transfer tunnel and hindered the electron transfer toward the surface of electrode (Jia et al., 2014; Han et al., 2013; Wei et al., 2010; Yu et al., 2013). As shown in Fig. 2B, the calibration curve revealed that there was a good linear correlation between DPV peak currents and the logarithm of CA125 concentrations in the range from 0.1 U mL^{-1} to 200 U mL^{-1}. The linear equation was $Y = 3.230 - 0.366X$ with correlation coefficient of 0.993 and the limit of detection (LOD) of 0.01 U mL^{-1} at signal-to-noise ratio of 3. The CA125 level in healthy human serum was less than 35 U mL^{-1}, thus the proposed immunosensor could be used for the testing of CA125 with the features of low detection limit, high detection accuracy and sensitivity.

The performance comparison between our proposed immunosensor and immunosensors reported in literature was shown in Table S1. The reported immunosensors adopted various methods including electrochemical immunoassay, electrochemiluminescence immunoassay and chemiluminescence immunoassay for the detection of CA125. As shown in Table S1, the linear detection range of our proposed immunosensor was wider than the other immunosensors. The LOD of our proposed immunosensor was lower than the reported immunosensor except for the immunosensor reported in literature of Guo et al. (2013). The reason was that Au@Pd core-shell nanoparticles could provide higher electrocatalytic activity than Au nanoparticles according to the literature of Guo et al. (2013), but our proposed immunosensor took shorter incubation time than the literature of Guo et al. (2013). Our proposed immunosensor and the literature of Torati et al. (2017) adopted one-step electrochemical technique while the other immunosensors in Table S1 employed sandwich technique. Compared to one-step electrochemical technique, the sandwich-type immunosensors needed more complex steps. The incubation time of sandwich-type immunosensors was between 180 s and 60 min, but it took additional time for the immobilization of the secondary antibody. Hence, one-step electrochemical technique was more suitable for POCT of CA125. As a result, the comparison results illustrated that our proposed immunosensor had relatively low LOD, wide linear range and short detection time.

3.5. Reproducibility, reliability and stability of immunosensor

To illustrate the intra-assay and inter-assay reproducibility and reliability of our proposed immunosensor, 1 U mL^{-1} CA125 was tested three times with three immunosensors. The relative standard deviation (RSD) was 2.57% and 4.77%, respectively, indicating good reproducibility and reliability. In order to verify the stability of proposed immunosensor, immunosensors were saved in the fridge at 4 °C for fortnight and tested in the same testing condition with 6.29% decrease of DPV current response. It showed that our proposed immunosensor had good stability.

3.6. Application in analysis of serum samples

In order to explore the clinical analytical performance of our proposed immunosensor, quality control serum samples were assayed. Under optimal conditions, the samples with known concentration from 2 U mL^{-1} to 64 U mL^{-1} were tested three times to get calibration curve by immunosensor, as well as also by ELISA as contrast (The result got by ELISA method was shown in Fig S4.). The linear calibration curve was shown in Fig. 3. The linear equation was $Y = 3.290 - 0.974X$. The correlation coefficient was 0.984 and the RSD was less than 4.6%. Eight quality control serum samples were measured three times with eight immunosensors and ELISA method. The comparison between the results obtained by immunosensor and ELISA method were shown in Table 1. The relative error was less than 8.05%, which indicated acceptable agreement between these two methods. Hence, our proposed immunosensor had good clinical analytical performance.

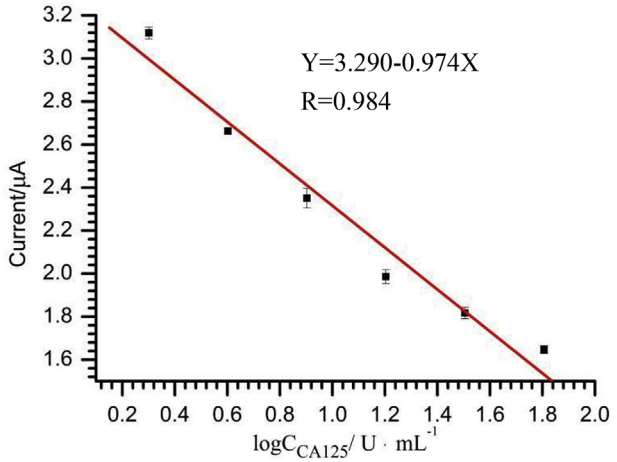

Fig.3. The linear calibration curve of samples with known concentration of CA125 from 2 U mL^{-1} to 64 U mL^{-1} (2 U mL^{-1}, 4 U mL^{-1}, 8 U mL^{-1}, 16 U mL^{-1}, 32 U mL^{-1},64 U mL^{-1}) tested three times with immunosensor.

Table 1
Quality control serum samples measured with our proposed immunosensor and ELISA method.

Sample No.	Our proposed method (U mL^{-1})	ELISA method (U mL^{-1})	Relative error (%)
1	12.94	12.54	3.19
2	17.72	17.12	3.50
3	28.05	26.34	6.49
4	60.27	62.84	−4.09
5	157.9	166.4	−5.11
6	300.6	278.2	8.05
7	295.1	304.7	−3.15
8	547.0	561.5	−2.58

3.7. The potential of POCT application

The POCT application potential of our proposed immunosensor was demonstrated here. Firstly, the immunosensor was fabricated on pure cellulose paper. Due to the the advantages of low cost, disposability, good biocompatibility and easy availability, the paper-based immunosensor could be used as disposables. Secondly, screen-printing technology had the advantages of low cost and simple fabrication process, which can be used for mass production of paper-based immunosensor. Thirdly, rGO/Thi/AuNPs nanocomposites modified immunosensor could provide high sensitivity and accuracy for the detection of CA125. Finally, our immunosensor had simple detection process and short detection time less than 25 min including the incubation time of CA125 antibody and antigen (20 min) and electrochemical detection time (160 s). Hence, our proposed immunosensor was very suitable for POCT of CA125.

4. Conclusion

In this article, a novel electrochemical immunosensor based on rGO/Thi/AuNPs nanocomposites was successfully developed for the sensitive determination of CA125. The testings of CA125 were performed on CHI 660E electrochemical workstation. Simple screen-printing technology and disposable pure cellulose paper were used for the fabrication of immunosensor. The rGO/Thi/AuNPs nanocomposites were synthesized for CA125 antibody immobilization and detection signal amplification. The detection of CA125 was based on the principle that the immunocomplex formed by specific binding of CA125 antibody and antigen could reduce the current responses of thionine, which was proportional to the corresponding concentration of CA125 antigen. The experiment results showed that the linear range of CA125 was from 0.1 U mL^{-1} to 200 U mL^{-1} with the limit of detection (LOD) of 0.01 U mL^{-1} and corresponding correlation coefficient of 0.993 at signal to noise of 3. There had acceptable relative error between the proposed immunosensor and ELISA method in clinical diagnosis. With the advantages of low cost, short detection time, disposability, low LOD, wide linear range, high sensitivity and accuracy, our proposed immunosensor could be used for POCT of tumor markers and had the potential for disease screening in remote region.

Declaration of interests

The authors declare that they have no known competing financial interests or personal relationships that could have appeared to influence the work reported in this paper.

The authors declare the following financial interests/personal relationships which may be considered as potential competing interests:

There is no competing financial interests or personal relationships that could have appeared to influence the work reported in this paper.

CRediT authorship contribution statement

Yan Fan: Conceptualization, Funding acquisition, Methodology, Supervision, Writing - original draft, Writing - review & editing. **Shengyu Shi:** Software, Validation. **Junshuang Ma:** Resources, Investigation, Writing - review & editing. **Yaohua Guo:** Formal analysis, Project administration.

Acknowledgements

This work was sponsored by the Key Research Program of HeBei Province (No.172777141) and the doctorial innovation funds of Tangshan university (No.1401804).

Appendix A. Supplementary data

Supplementary data related to this article can be found at https://doi.org/10.1016/j.bios.2019.03.063.

References

Al-Ogaidi, I., Gou, H., Aguilar, Z.P., Guo, S., Melconian, A.K., Al-Kazaz, A.K., 2014. Detection of the ovarian cancer biomarker ca-125 using chemiluminescence resonance energy transfer to graphene quantum dots. Chem. Commun. 50 (11), 1344–1346.

Babamiri, B., Hallaj, R., Salimi, A., 2017. Ultrasensitive electrochemiluminescence immunoassay for simultaneous determination of ca125 and ca15-3 tumor markers based on pamam-sulfanilic acid-ru(bpy)3(2+) and pamam-cdte at cds nanocomposite. Biosens. Bioelectron. 99, 353–360.

Bolotin, K.I., Sikes, K.J., Jiang, Z., Klima, M., Fudenberg, G., Hone, J., Kima, P., Stormer, H.L., 2008. Ultrahigh electron mobility in suspended graphene. Solid State Commun. 146 (9), 351–355.

Bruzewicz, D.A., Reches, M., Whitesides, G.M., 2008. Low-cost printing of poly(dimethylsiloxane) barriers to define microchannels in paper. Anal. Chem. 80 (9), 3387.

Chu, W., Chen, Y., Liu, W., Zhao, M., Li, H., 2017. Paper-based chemiluminescence immunodevice with temporal controls of reagent transport technique. Sensor. Actuator. B Chem. 250, 324–332.

Dungchai, W., Chailapakul, O., Henry, C.S., 2011. A low-cost, simple, and rapid fabrication method for paper-based microfluidics using wax screen-printing. Analyst 136 (1), 77–82.

Fan, Y., Wang, Y., Liu, J., Luo, J., Xu, H., Xu, S., Cai, X., 2016. Development of portable device for point-of-care testing of tumor marker. Chin. J. Anal. Chem. 44 (7), 1148–1154.

Fan, Y., Liu, J., Wang, Y., Luo, J., Xu, H., Xu, S., Cai, X., 2017. A wireless point-of-care testing system for the detection of neuron-specific enolase with microfluidic paper-based analytical devices. Biosens. Bioelectron. 95, 60–66.

Francis, L., 2016. Tumor necrosis factor-α and interferon-γ stimulate muc16 (ca125) expression in breast, endometrial and ovarian cancers through nfκb. Oncotarget 7 (12), 14871–14884.

Gasparotto, G., Costa, João Paulo C., Costa, P.I., Zaghete, M.A., Mazon, T., 2017. Electrochemical immunosensor based on zno nanorods-au nanoparticles nanohybrids for ovarian cancer antigen ca-125 detection. Mater. Sci. Eng. C 76, 1240.

Guo, A., Wu, D., Ma, H., Zhang, Y., Li, H., Du, B., Wei, Q., 2013. An ultrasensitive enzyme-free electrochemical immunosensor for ca125 using au@pd core–shell nanoparticles as labels and platforms for signal amplification. J. Mater. Chem. B 1 (33), 4052–4058.

Guo, Z., Qiu, L., Zhang, F., Yang, F., Zhao, L., Zhang, Y., Zhu, X., Qiu, N., 2003. Diagnostic and prognostic values of serum ca125, nse, ct levels in patients with lung cancer. Chin. J. Lung Canc. 6 (3), 206–208.

Han, J., Ma, J., Ma, Z., 2013. One-step synthesis of graphene oxide–thionine–Au nanocomposites and its application for electrochemical immunosensing. Biosens. Bioelectron. 47, 243–247.

Hu, J., Wang, S., Wang, L., Li, F., Pingguan-Murphy, B., Lu, T., Xu, F., 2015. Advances in paper-based point-of-care diagnostics. Biosens. Bioelectron. 54, 585–597.

Jia, X., Liu, Z., Liu, N., Ma, Z., 2014. A label-free immunosensor based on graphene nanocomposites for simultaneous multiplexed electrochemical determination of tumor markers. Biosens. Bioelectron. 53, 160–166.

Johariahar, M., Rashidi, M.R., Barar, J., Aghaie, M., Mohammadnejad, D., Ramazani, A., Karamia, P., Coukosd, G., Omidia, Y., 2015. An ultra-sensitive impedimetric immunosensor for detection of the serum oncomarker ca-125 in ovarian cancer patients. Nanoscale 7 (8), 3768–3779.

Klasner, S.A., Price, A.K., Hoeman, K.W., Wilson, R.S., Bell, K.J., Culbertson, C.T., 2010. Paper-based microfluidic devices for analysis of clinically relevant analytes present in urine and saliva. Anal. Bioanal. Chem. 397 (5), 1821–1829.

Lei, G., Yu, J., Ge, S., Mei, Y., 2014. Lab-on-paper-based devices using chemiluminescence and electrogenerated chemiluminescence detection. Anal. Bioanal. Chem. 406 (23), 5613–5630.

Li, L., Li, W., Ma, C., Yang, H., Ge, S., Yu, J., 2014a. Paper-based electrochemiluminescence immunodevice for carcinoembryonic antigen using nanoporous gold-chitosan hybrids and graphene quantum dots functionalized au@pt. Sensor.

Actuator. B Chem. 202 (4), 314–322.
Li, W., Li, L., Ge, S., Song, X., Lei, G., Mei, Y., Yu, J.H., 2014b. Multiplex electrochemical origami immunodevice based on cuboid silver-paper electrode and metal ions tagged nanoporous silver–chitosan. Biosens. Bioelectron. 56 (1), 167–173.
Li, W., Li, L., Li, S., Wang, X., Li, M., Wang, S., Yu, J., 2013. 3D origami electrochemiluminescence immunodevice based on porous silver-paper electrode and nanoporous silver double-assisted signal amplification. Sensor. Actuator. B Chem. 188 (11), 417–424.
Lu, J., Liu, S., Ge, S., Yan, M., Yu, J., Hu, X., 2012. Ultrasensitive electrochemical immunosensor based on au nanoparticles dotted carbon nanotube–graphene composite and functionalized mesoporous materials. Biosens. Bioelectron. 33 (1), 29–35.
Lu, W., Ge, J., Tao, L., Cao, X., Dong, J., Qian, W., 2014. Large-scale sythesis of ultrathin Au-Pt nanowires assembled on thionine/graphene with high conductivity and sensitivity for electrochemical immunosensor. Electrochim. Acta 130, 335–343.
Martinez, A.W., Phillips, S.T., Carrilho, E., Rd, T.S., Sindi, H., Whitesides, G.M., 2008. Simple telemedicine for developing regions: camera phones and paper-based microfluidic devices for real-time, off-site diagnosis. Anal. Chem. 80 (10), 3699.
Nery, E.W., Kubota, L.T., 2013. Sensing approaches on paper-based devices: a review. Anal. Bioanal. Chem. 405 (24), 7573–7595.
Nguyen, L., Cardenas-Goicoechea, S.J., Gordon, P., Curtin, C., Momeni, M., Chuang, L., Fishman, D., 2013. Biomarkers for early detection of ovarian cancer. Women's Health 9 (2), 171–187.
Olkkonen, J., Lehtinen, K., Erho, T., 2010. Flexographically printed fluidic structures in paper. Anal. Chem. 82 (24), 10246.
Peng, H.P., Hu, Y., Liu, A.L., Chen, W., Lin, X.H., Yu, X.B., 2014. Label-free electrochemical immunosensor based on multi-functional gold nanoparticles–polydopamine–thionine–graphene oxide nanocomposites film for determination of alpha-fetoprotein. J. Electroanal. Chem. 712, 89–95.
Rong, Q., Feng, F., Ma, Z., 2016. Metal ions doped chitosan-poly(acrylic acid) nanospheres: synthesis and their application in simultaneously electrochemical detection of four markers of pancreatic cancer. Biosens. Bioelectron. 75, 148–154.
Santhiago, M., Kubota, L.T., 2013. A new approach for paper-based analytical devices with electrochemical detection based on graphite pencil electrodes. Sensor. Actuator. B Chem. 177 (2), 224–230.
Santillan, A., Garg, R., Zahurak, M.L., Gardner, G.J., Giuntoli, R.L., Armstrong, D.K., Bristow, R.E., 2005. Risk of epithelial ovarian cancer recurrence in patients with rising serum ca-125 levels within the normal range. J. Clin. Oncol. Off. J. Am. Soc. Clin. Oncol. 23 (36), 9338.
Songjaroen, T., Dungchai, W., Chailapakul, O., Henry, C.S., Laiwattanapaisal, W., 2012. Blood separation on microfluidic paper-based analytical devices. Lab Chip 12.
Torati, S.R., Kasturi, K.C.S.B., Lim, B., Kim, C.G., 2017. Hierarchical gold nanostructures modified electrode for electrochemical detection of cancer antigen ca125. Sensor. Actuator. B Chem. 243, 64–71.
Wang, Y., Xu, H., Luo, J., Liu, J., Wang, L., Fan, Y., Yan, S., Yang, Y., Cai, X., 2016. A novel label-free microfluidic paper-based immunosensor for highly sensitive electrochemical detection of carcinoembryonic antigen. Biosens. Bioelectron. 83, 319–326.
Wei, Q., Mao, K., Wu, D., Dai, Y., Yang, J., Du, B., Yang, M., Li, H., 2010. A novel label-free electrochemical immunosensor based on graphene and thionine nanocomposite. Sensor. Actuator. B Chem. 149 (1), 314–318.
Wu, Y., Xue, P., Hui, K., Kang, Y., 2014. A paper-based microfluidic electrochemical immunodevice integrated with amplification-by-polymerization for the ultrasensitive multiplexed detection of cancer biomarkers. Biosens. Bioelectron. 52 (4), 180–187.
Xiao, Q., Lin, J.M., 2015. Advances and applications of chemiluminescence immunoassay in clinical diagnosis and foods safety. Chin. J. Anal. Chem. 43 (6), 929–938.
Yan, J., Ma, C., Hu, X., He, Q., 2014. Fabrication techniques of microfluidic paper-based chips and their applications. Prog. Chem. 26 (1), 167–177.
Yu, Shu, Wei, Q., Du, B., Wu, D., Li, H., Yan, L., Ma, H., Zhang, Y., 2013. Label-free immunosensor for the detection of kanamycin using Ag@Fe3O4 nanoparticles and thionine mixed graphene sheet. Biosens. Bioelectron. 48, 224–229.
Zhang, A.L., Zha, Y., 2012. Fabrication of paper-based electrochemical device using printed circuit technology. AIP Adv. 2 (2), 022171.